Neuroepigenetics 6 (2016) 26–31

Contents lists available at ScienceDirect

Neuroepigenetics

journal homepage: www.elsevier.com/locate/nepig

Increased 5-hydroxymethylation levels in the sub ventricular zone of the Alzheimer's brain

Diego Mastroeni [a,b,c,*], Leonidas Chouliaras [c,d], Daniel L. Van den Hove [c], Jennifer Nolz [a], Bart P.F. Rutten [c], Elaine Delvaux [a], Paul D. Coleman. [a,b]

[a] ASU-Banner Neurodegenerative Disease Research Center, Biodesign Institute and School of Life Sciences, Arizona State University, Tempe, AZ
[b] Banner Sun Health Research Institute, 10515 West Santa Fe Drive, Sun City, AZ, 85351, USA
[c] School for Mental Health and Neuroscience (MHeNS), Department of Psychiatry and Neuropsychology, Faculty of Health, Medicine and Life Sciences, European Graduate School of Neuroscience (EURON), Maastricht University Medical Centre, Maastricht, The Netherlands
[d] Department of Psychiatry, University of Oxford, Warneford Hospital, OX3 7JX, Oxford, UK

ARTICLE INFO

Article history:
Received 17 November 2015
Received in revised form 25 March 2016
Accepted 27 April 2016

ABSTRACT

The subventricular zone (SVZ) is a site of neurogenesis in the aging brain, and epigenetic mechanisms have been implicated in regulating the "normal" distribution of new nerve cells into the existing cellular milieu. In a case-control study of human primary SVZ cultures and fixed tissue from the same individuals, we have found significant increases in DNA hydroxymethylation levels in the SVZ of Alzheimer's disease patients compared with nondiseased control subjects. We show that this increase in hydroxymethylation directly correlates to an increase in cellular proliferation in Alzheimer's disease precursor cells, which implicates the hydroxymethylation tag to a higher degree of cellular proliferation.

1. Introduction

It is well established that the act of self-renewal, particularly during neuronal differentiation, requires many intrinsic and extrinsic factors. Neurogenesis and its incorporation into the existing neuronal circuitry are a central event in the process of efficient aging (Lazarov et al., 2010). It has been shown that the rate of neurogenesis decreases as a function of age (Riddle and Lichtenwalner, 2007; Conover and Shook, 2011), contrary of what has been observed in Alzheimer's disease (AD) (Jin et al., 2004a, 2004b). Unlike normal aging, the AD brain is subjected to many environmental stimulants known to induce neurogenesis, that is, amyloid (Lopez-Toledano and Shelanski, 2004), donepezil (Kotani et al., 2008), memantine (Jin et al., 2006), nonsteroidal anti-inflammatory drugs (Monje et al., 2002), brain trauma (Chen et al., 2003b), and statins (Chen et al., 2003a), to name a few. Because the environment inside and outside the cell directly affects epigenetic mechanisms that regulate the expression of multipotent genes (Feil and Fraga, 2011; Dao et al., 2014), the increased multipotency observed in AD (Fitzsimons et al., 2014) implicates epigenetic mechanisms like 5-hydroxymethylation (Dao et al., 2014).

Epigenetic mechanisms encompass a wide array of functional roles, which in due course lead to the repression or expression of genes. Although the existence and biological functions of active methylation (generally mediating gene repression) and demethylation (generally inducing gene expression) are still in its infancy, 5hmC has been implicated in active DNA demethylation (Zhang et al., 2012), particularly in multipotent genes (Szulwach et al., 2011). The 5-hydroxymethylcytosine (5hmeC) mark is an oxidized form of 5-methylcytosine (5meC) (Tahiliani et al., 2009). Oxidation of 5meC to 5hmeC is catalyzed by a family of proteins (ten-eleven translocation) that have also been implicated in the regulation and maintenance of multipotency (Tahiliani et al., 2009; Freudenberg et al., 2012). Because the subventricular zone (SVZ) is a site of neurogenesis and gliogenesis (Ming and Song, 2011), our data identify an epigenetic mechanism that could account for the increase in multipotency observed in AD. These data provide the foundation for future gene-specific studies and a possible therapeutic approach to neuronal differentiation in AD SVZ.

2. Materials and methods

2.1. Autopsy brain tissue

Brain tissue was obtained through the Sun Health Brain and Body Donation Program (Sun City, AZ). Specimens at autopsy were collected under institutional review board–approved protocols and informed

* Corresponding author at: Biodesign Institute, Arizona State University, Tempe, AZ, 85287, United States.
E-mail address: dmastroe@asu.edu (D. Mastroeni).

http://dx.doi.org/10.1016/j.nepig.2016.04.002

Table 1
Characteristics of cases used for quantitative assessment

Sex	Age expired	PMI	Control	AD	Braak score
F	90	3	Yes	No	II
M	86	2.5	Yes	No	II
M	86	2.66	Yes	No	II
F	90	2.5	Yes	No	II
M	83	2.16	Yes	No	III
F	96	3	Yes	No	III
F	86	2.5	No	Yes	IV
F	91	4.5	No	Yes	IV
M	85	5.75	No	Yes	IV
F	85	3.16	No	Yes	VI
M	79	1.83	No	Yes	VI
M	86	2.83	No	Yes	VI

consents that permitted use of the samples for research by the investigators. At expiration, subject ages ranged from 79 to 96 years old ($N = 12$), with a mean of 86.9 ± 1.1 (SEM) years. Postmortem intervals for the subjects averaged 3 hours ± 3 minutes. Diagnoses of patient condition included AD ($n = 6$) and neurologically/pathologically normal for age ($n = 6$) (Table 1). Subjects included in this study received antemortem evaluation by board-certified neurologists and postmortem evaluation by a board-certified neuropathologist. Evaluations and diagnostic criteria followed consensus guidelines for National Institute on Aging Alzheimer's Disease Centers.

After brain removal, gross surface neuropathological abnormalities were documented, 1-cm–thick frontal slabs were cut and photographed, and the slabs were bisected into hemispheres. Small blocks that included superior-lateral periventricular white matter were immediately dissected from right hemisphere slabs and processed for primary cell culture or for fixation and detailed immunohistochemical study (see below).

2.2. SVZ dissection, tissue dissociation, and primary cell culture

As previously published (Leonard et al., 2009), SVZ cultures were dissected from the superior lateral wall of the lateral ventricle, from the most anterior aspect of the lateral ventricle to approximately 3 cm posterior to that point. These dissections typically included approximately 1 cm of white matter but specifically excluded any striatal gray matter. For parallel, control cultures, neocortical tissue blocks from the same cases were dissected from frontal and/or parietal regions. These latter slabs always included all adjoining subcortical white matter, except for a 2-cm margin around the lateral ventricle that contained the SVZ. Eliminating the SVZ from these samples provided a control to evaluate whether neurosphere development in our SVZ cultures derived from the SVZ or from surrounding periventricular tissue necessarily included in the SVZ dissections.

Tissue was quickly transported in ice-cold Hibernate A medium (BrainBits, LLC, Springfield, IL) to a sterile laminar flow hood, mechanically dissociated into 1–2 mm pieces, and digested with 0.25% trypsin (Irvine Scientific, Santa Ana, CA) and 0.1% DNAse (Sigma, St. Louis, MO) in a shaking water bath at 30°C. Digestion was stopped with fetal bovine serum. After passing the cell and tissue suspension through progressively finer metal screens, it was diluted with complete Dulbecco modified Eagle medium (DMEM) (minus phenol red). Complete DMEM consisted of 500 mL DMEM (high glucose, plus or minus phenol red, as noted; Invitrogen-Gibco, Carlsbad, CA), 50 mL fetal bovine serum (Gemini Bio-Products, West Sacramento, CA), 10 mL HEPES (Irvine Scientific), 5 mL sodium pyruvate (Mediatech Cellgro, Herndon, VA), 5 mL penicillin/streptomycin (Invitrogen-Gibco), and 0.5 mL gentamycin (Irvine Scientific). Cells and debris were separated using 50% Percoll gradient (Amersham/GE Healthcare, Piscataway, NJ) centrifugation (13,000 rpm; refrigerated). The first layer of myelin and debris was discarded. The second layer of the gradient, which is rich in microglia and astrocytes (Lue et al., 1996) but also proved to be the most optimal source for neurospheres, was aspirated, washed, pelleted, gently triturated, washed a second time, resuspended in complete DMEM (plus phenol red), and transferred to a 75-mL tissue culture flask (Nunc, Rochester, NY).

Flasks with suspended cells were left undisturbed for 2–24 hours in a tissue culture incubator maintained at 37°C/7% CO_2. As previously reported (Lue et al., 1996), some 98% of microglia became adherent under these conditions, such that culture supernatants that were relatively free of microglia could be transferred to a second set of 75-mL flasks for plating. To estimate viability and density of the cells remaining in suspension, 50-μL aliquots of cell suspension were subjected to trypan blue exclusion counting using a hemocytometer.

The secondary flasks were left undisturbed, except for weekly medium replacement with complete DMEM, for 1–3 weeks in tissue culture incubators maintained at 37°C with 7% CO_2, after which a portion of the supernatant was seeded into various receptacles depending on experimental requirements. When flasks became confluent, neurospheres and lightly adherent cell clusters were mechanically dislodged by brief gentle shaking, gently pelleted and triturated, and plated into a new flask; neurospheres were not intentionally dissociated during passage. Characterization studies typically used 6- or 12-well uncoated tissue culture plates (Corning, Lowell, MA) or plates and culture dishes coated with 10 μg/mL poly-L-lysine (Sigma) or a combination of poly-L-lysine /10 μg/mL mouse laminin I (ATCC, Manassas, VA).

2.3. Immunohistochemistry and immunocytochemistry

For immunohistochemical analysis of tissue sections, periventricular white matter/SVZ blocks were collected at autopsy in the same manner as that for cell culture. Tissue blocks were immersion-fixed at 4°C for 24–36 hours in freshly made 4% paraformaldehyde/0.1 mol/L PO_4 (phosphate buffer, PB). The blocks were then washed extensively in PB, cryoprotected in 30% sucrose, sectioned serially at 20 μm or 40 μm on a cryostat, and stored at −20°C in ethylene glycol/glycerol/PB solution until needed.

2.3.1. 3,3'-diaminobenzidine immunohistochemistry

Forty-micrometer free floating sections were washed in phosphate-buffered saline Triton X-100, blocked in 1% hydrogen peroxide followed by 1-hour incubation in 3% bovine serum albumin (BSA), and then incubated at 4°C overnight in primary antibody (5hmeC; Active Motif, Carlsbad, CA; 1:5000 dilution) solutions containing 0.25% BSA. After incubation, the sections were washed; incubated in biotinylated, species-specific secondary antibodies (Vector) for 2 hours at room temperature (RT); washed 3× in phosphate-buffered saline Triton X-100; and incubated in avidin-biotin complex (Pierce) for 30 min. Following incubation with avidin-biotin complex, sections were washed 2× in 50 mmol/L Tris buffer and immersed in 3,3'-diaminobenzidine solution (500 μL 5 mg/mL 3,3'-diaminobenzidine, 2 mL saturated nickel, 10 μL 1% H202, fill to 50 mL with 50 mmol/L Tris buffer) for no longer than 10 minutes, followed 2 quick rinses in 50 mmol/L Tris to stop the reaction. AD and nondiseased (ND) sections were immunoreacted simultaneously using Netwells in well-less plates. Sections were mounted with Permount (Pierce).

2.3.2. Fluorescence immunohistochemistry

Briefly, extensively washed 40-μmol/L sections were blocked with 3% normal goat serum (NGS)/0.1% Triton X-100 and then incubated with rabbit anti-human 5hmeC, diluted 1:5000 (Active Motif, Carlsbad, CA) for 24 hours at 4°C. The diluent for all solutions and washes was 0.05 mol/L Tris-buffered saline, pH 7.4. After 3 washes, the sections were incubated with goat anti-rabbit Alexa-Fluor 488–conjugated secondary antibody (1:1500; Invitogen/Molecular Probes) for 2 hours at room temperature, washed, mounted on microscope slides, and coverslipped with Vectashield mounting medium (Vector Laboratories, Burlingame, CA). All washes included 1% NGS and 0.1%

Triton in Tris-buffered saline. Deletion of primary antibody or incubation with hydroxymethylated nucleotides (5-hydroxymethyl dCTP; Zymo Research, Irvine, CA) resulted in abolition of specific immunoreactivity. Adjacent serial sections were stained with cresyl violet for cell layer identification and verification that the ependymal layer of the adjacent immunofluorescent sections was intact. For some sections, nuclei were counterstained with 4′,6′-diamidino-2-phenylindole (DAPI; Invitrogen) before mounting.

2.3.3. Fluorescence immunocytochemistry

For immunocytochemical analysis of cell cultures, medium was aspirated, and cultures were briefly washed with either RT phosphate-buffered saline (PBS) (Invitrogen-Gibco) or 37°C PEM (100 mmol/L PIPES, 2 mmol/L EGTA, l mmol/L $MgSO_4$, pH 6.9) and then fixed with RTacetone-ethanol (1:1 for 15 minutes at 4°C). The cells were washed briefly, and nonspecific binding was blocked with either 3% NGS (Sigma) or 1% BSA (Sigma)/0.1% Triton for 45 minutes at room temperature. Cultures were then incubated with primary antibody diluted in 1% NGS/PBS for 1 hour at room temperature. Following 3 brief washes, cells were incubated with species-appropriate secondary antibodies conjugated with Alexa-Fluor 488 or Alexa-Fluor 568 fluorophores (Invitrogen/Molecular Probes) for 1 hour at room temperature in the dark. Washes throughout all steps were with 1× PBS; as with tissue sections, we observed no specific immunostaining when primary antibodies were deleted.

Immunostained periventricular white matter/SVZ tissue sections and cell cultures were examined on Olympus IX70 microscopes equipped with epifluorescence illumination or confocal laser scanning using argon and krypton lasers (IX70). Findings were documented photographically with Olympus DP-71 color digital cameras or, for confocal microscopy, by Fluoview software (Olympus). Contrast and brightness adjustments and overlay compositing were done with Adobe Photoshop CS3.

2.4. Slot blot

DNA was isolated from cultured cells using the QIAamp DNA mini kit (Qiagen) and quantified using Quant-iT PicoGreen dsDNA Assay Kit (Life Technologies). One microgram of DNA was denatured using 0.4 mol/L NaOH. Samples were then heated to 100°C for 10 minutes to ensure complete denaturation. Samples were then neutralized by adding an equal volume of 2 mol/L ammonium acetate, pH 7.0, to the target DNA solution. Samples were loaded onto prewet (6× SSC) Hybond-ECL nitrocellulose membrane loaded into a 48-well Bio-Dot SF (slot format) microfiltration unit (Bio-Rad). With the vacuum off, 500 μL of denatured DNA is loaded and pulled through by gravity filtration, followed by gentle vacuum. Membrane was removed and allow to air dry for 30 minutes at RT. Once dry, membrane was placed between 2 pieces of filter paper and baked under vacuum at 80°C for 2 hours. Membrane was then blocked for 2 hours in 5% milk in dot blot buffer (20 mmol/L Tris, .05% Tween-20), washed 1× in dot blot buffer, and incubated in primary antibody (5-hmec, 1:10,000) for 2 hours at RT in dot blot buffer and 5% milk. Membrane was then washed 5× for 5 minutes and incubated in horseradish peroxidase–conjugated secondary antibody (anti-rabbit, 1:5000) for 1 hour at RT in dot blot buffer and 5% milk, followed by 5 washes in dot blot buffer for 5 minutes. Membranes were incubated in ECL reagent and imaged on AlphaEaseFC (Alpha Innotech). After imaging, membranes were washed with dH_2O and placed in .025% methylene blue for 2 minutes, washed 1× in dH_2O, and imaged on AlphaEaseFC.

2.5. WST-1 assay

Cultured cells from the human SVZ were isolated as described above. Per manufacturer's instructions (ABCAM), cells were grown 1×10^4 cells/well in a 96-well microtiter plate in a final volume of 100 μL of complete media (described above). After 72 hours, 10 μL of WST-1 reagent was added to each well, including blank wells with no cells (media and WST-1 reagent only). Cells were incubated in WST-1 reagent for 30 minutes in a 37°C incubator and for 1 minute on a shaking platform. Plates were read using a Wallac microplate reader at an optical density of 440 nm. All experiments were done in triplicate.

2.6. Statistical analyses/quantification

Bright field/fluorescence intensity analysis was performed using ImageJ software (ImageJ, US National Institutes of Health, Bethesda, MD; imagej.nih.gov/ij/). Intensity measurements were corrected for background differences by dividing the measured intensities with the average intensity of a background region. Significance was determined using a 2-tailed Student t test and declared significant at a P value < .05.

3. Results

3.1. Increased 5-hydroxymethylation immunoreactivity in the SVZ of Alzheimer's brain in vivo

Quantification of 5hmeC immunoreactivity in layer III of the SVZ showed a significant increase in immunoreactivity in AD compared with age-matched controls (Fig. 1). Layer I (ependymal cell layer), the innermost cell layer of the SVZ, showed no significant difference in immunoreactivity between AD and ND cases ($P = .21$; Fig. 1A vs. B). Similarly, layer II (hypocellular gap), a region which contains little in the way of cell bodies but does contain astrocytic processes, revealed no significant difference in immunoreactivity between AD and ND cases ($P = .008$, Fig. 1A vs. B), although control cases were trending toward higher 5hmeC levels (Fig. 1A). Analysis of layer III, which contained multipotent cells, delineated by the presence of GFAP delta positive immunoreactivity (Leonard et al., 2009), revealed a significant increase when comparing AD with control samples ($P < .001$). Layer IV, the transition zone between the multipotent astrocytes and parenchyma, showed no significant difference between groups ($P = .19$). To enable correction for possible cell loss, the total number of cells in the SVZ were counted, but no significant difference was observed ($P = .22$) and therefore no correction was needed.

3.2. Quantification of 5hmeC immunoreactivity in SVZ, both in vivo (brain tissue) and in vitro (primary cultures) from matching AD and ND cases

In vivo data in a case-control study showed significantly less (2-tail, t test $P = 4.4e\text{-}5$) 5hmeC levels (average gray value of pixels, normalized to cell number intensity DAPI) in the control (Fig. 2, A1) compared with AD SVZ (Fig. 2, A2). Similarly, primary cultures of the same individuals show significantly less ($P = .002$) 5hmeC immunoreactivity in ND neurospheres (Fig. 2, B1) compared with AD (Fig. 2, B2). Slot blot analysis of nuclear DNA extracted form neurospheres and adherent cells from the SVZ revealed a global increase in 5hmeCs in AD (Fig. 2C–D), in line with the immunohistochemical experiments. These data show that both cultured cells and brain tissue from the same individuals behave similarly with respect to 5hmeC levels.

To determine whether 5 hydroxymethylation levels affect proliferation potential differentially in AD and ND cultured cells, WST-1 proliferation assays were performed. Fig. 3 shows a significant increase (2-tail, t test $P = 2.9$ E-07) in the proliferation potential in AD SVZ precursor cells compared with normal controls. Although correlative, these data indicate that an increase in 5-hydroxymethylation levels can predict an increase in proliferation in the SVZ of AD cultured precursor cells.

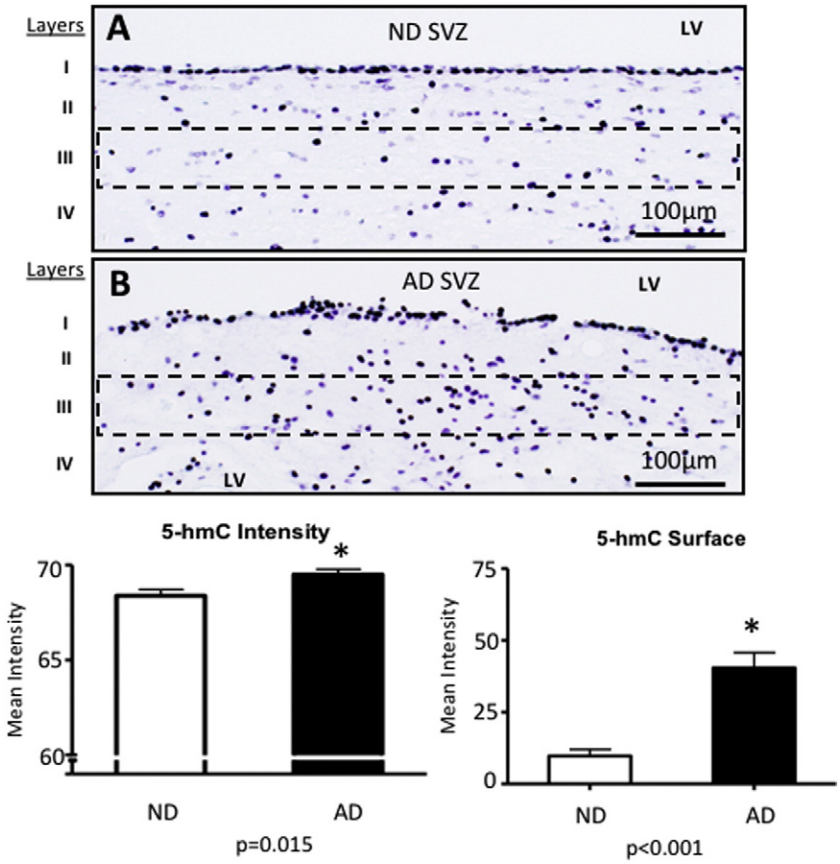

Fig. 1. Quantification of 5hmeC immunoreactivity in the SVZ of AD (n = 5) and ND (n = 5) brains. Representative photomicrograph analysis of ND SVZ (A) reveals significantly less immunoreactivity in layer III (boxed region) compared with AD cases (B). Bar graphs show the mean intensity for 5hmeC surface area (percentage of area within the delineated region above background), 2-tail *t* test, $P < .001$. Dashed lines indicate the delineated regions for analysis. *Significant difference; error bars were generated as standard error of the mean. LV, left ventricle.

4. Discussion

Stem cells have been proposed to provide the potential to revolutionize biomedicine in the next 2 decades. New research already shows that they can replace the lost nerve cells in Parkinson's disease (Politis and Lindvall, 2012), improve outcomes after heart attacks (Zakharova et al., 2010), rescue memory in mice with advanced AD (Yamasaki et al., 2007; Blurton-Jones et al., 2009), and ameliorate a host of other major human disorders. Although it was once believed that human stem cells were more or less the exclusive province of embryos, it is now clear that they persist into adulthood as adult progenitor stem cells. Indeed, studies conducted by our laboratory have shown that highly viable, adult progenitors can be isolated from the SVZ of postmortem brain and retained in culture for years (Leonard et al., 2009).

Because the SVZ is a site of neurogenesis in the aging brain (Riddle and Lichtenwalner, 2007) and epigenetic mechanisms have been implicated in regulating the "normal" distribution of new nerve cells into the existing cellular milieu (Ma et al., 2010), we tested relative 5hmeC levels in AD because of the critical role 5hmeC has in mediating the expression of multipotent genes (Navarro et al., 2014). In the AD SVZ, we determined that there was a significant increase in 5hmeC levels in layer III (Fig. 1A) compared with normal controls in vivo. We further tested 5hmeC levels in vitro in a set of AD and ND cases and found that both neurospheres and adherent precursor cells expressed higher levels of 5hmeC levels in AD compared with control. Finally, we show that this increase in 5hmeC levels correlate to higher degree of proliferation in culture. Although the sample size is relatively small, the complimentary data indicate that 5hmeC levels are consistent in vivo and in vitro, potentially identifying a model for further analysis.

We further mined the clinical data for an association between medications taken and a potential increase in cellular proliferation (data not shown), but no such association was found. This may be due to the small sample size or the overlap between medication (e.g., blood pressure and cholesterol medications) within subjects regardless of disease.

Over the past decade, intense investigation within the neurogenesis has indicated an increase in cellular proliferation in AD and in AD mouse models (Jin et al., 2004b; Boekhoorn et al., 2006; Yu et al., 2009; Mu and Gage, 2011; Perry et al., 2012; Marlatt et al., 2014), although the relevance of mouse models in recapitulating disease has been questioned (Kuhn et al., 2007). Although an increase in the number proliferating cells has been reported in glial, vascular, and neuronal precursor cells (reviewed in Fitzsimons et al., 2014), none have identified a causal mechanism. It has been previously reported that 5hmeC levels are linked to a higher degree of multipotency and cellular proliferation (Ficz et al., 2011; Navarro et al., 2014), and here, we make the case, although speculative, that the increase in proliferation in AD may be directly linked to the increase in 5hmeC levels. Undoubtingly, this increase in cellular proliferation would be advantageous in a disease like AD where neuronal loss is a prominent pathological feature. However, many of these same reports show that the number of proliferating cells does not increase in differentiated neurons in AD (Perry et al., 2012). Although the fact remains that neurogenesis is an important part of healthy aging, its role in disease is still unclear. The need for further manipulation studies of the 5hmeC mark, possibly through the actions of ten-eleven translocation

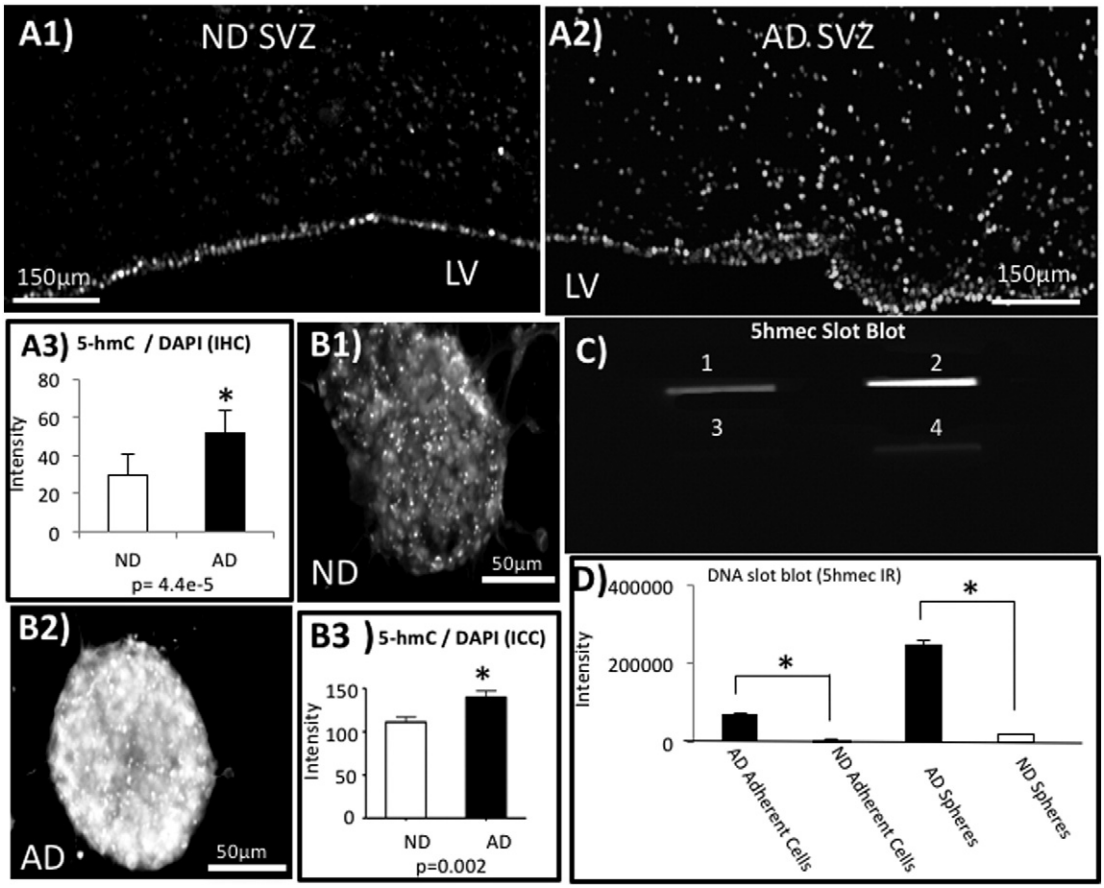

Fig. 2. Quantification of 5hmeC immunoreactivity in SVZ both in vivo (brain tissue) and in vitro (neurosphere primary cultures) from matching AD and ND cases. Control SVZ (A1) shows significantly less 5hmeC intensity compared with AD SVZ (A2). Bar graph (A3) shows quantification (5hmeC average gray value of pixels, normalized to cell number intensity DAPI immunoreactivity) of the immunohistochemical results. Similarly, primary cultures of the same individuals show significantly less 5hmeC immunoreactivity ($P = .002$) in ND neurospheres (B1) compared with AD (B2). Corresponding bar graph (B3) shows quantification of the immunocytochemical data. Slot blot analysis of nuclear DNA extracted from neurospheres and adherent cells from the SVZ reveals a global increase in 5hmeCs in AD (C), slot 1 (AD neurospheres), slot 3 (ND neurospheres), slot 2 (AD adherent cells), and slot 4 (ND adherent cells). Normalized 5hmeC levels to methylene blue signal reveal a significant increase in both AD spheres and adherent cells, 2-tail t test, $P = .001$ and $< .001$, respectively (D). *Significant difference ($P < .05$); error bars were generated as standard error of the mean.

proteins, which catalyze the conversion from 5meC to 5hmeC, may be an important cofactor in promoting cellular differentiation. The data presented here identify a potential model system for further studies in addressing the epigenetic mechanism(s) to promote cellular differentiation.

Acknowledgements

The authors declare no competing financial or conflict of interests. We are grateful to the Banner Sun Health Research Institute Brain and Body Donation Program of Sun City, AZ, for the provision of human

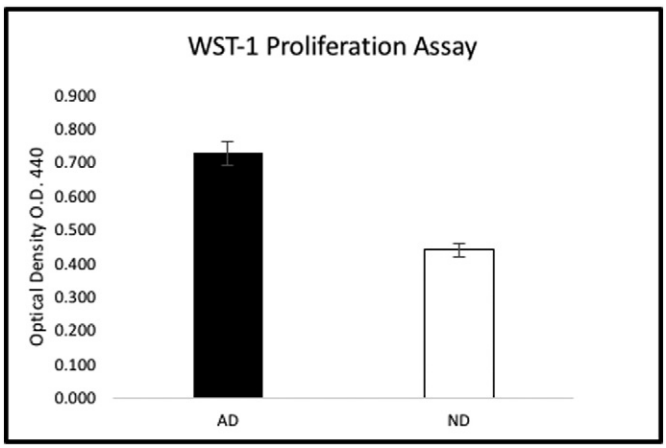

Fig. 3. WST-1 proliferation assay. Cultured precursor cells from AD and control brain were plated and incubated in WST-1 reagent, which is based on the cleavage of the tetrazolium salt WST-1 to formazan by cellular mitochondrial dehydrogenases. The reaction yields a color product indicative of the proliferation rate, which was significantly higher in the AD case vs. control sample. Error bars were generated as standard error of the mean.

brain samples. The Brain and Body Donation Program is supported by the National Institute of Neurological Disorders and Stroke (U24 NS072026 National Brain and Tissue Resource for Parkinson's Disease and Related Disorders), the National Institute on Aging (P30 AG19610 Arizona Alzheimer's Disease Core Center), the Arizona Department of Health Services (contract 211002, Arizona Alzheimer's Research Center), the Arizona Biomedical Research Commission (contracts 4001, 0011, 05-901, and 1001 to the Arizona Parkinson's Disease Consortium), and the Michael J. Fox Foundation for Parkinson's Research. This work was supported by NIRG-14-321390 and ADHS14-080000 FY2015 to DM.

References

Blurton-Jones, M., Kitazawa, M., Martinez-Coria, H., Castello, N.A., Muller, F.J., Loring, J.F., Yamasaki, T.R., Poon, W.W., Green, K.N., LaFerla, F.M., 2009. Neural stem cells improve cognition via BDNF in a transgenic model of Alzheimer disease. Proc. Natl. Acad. Sci. U. S. A. 106, 13594–13599.

Boekhoorn, K., Joels, M., Lucassen, P.J., 2006. Increased proliferation reflects glial and vascular-associated changes, but not neurogenesis in the presenile Alzheimer hippocampus. Neurobiol. Dis. 24, 1–14.

Chen, J., Zhang, Z.G., Li, Y., Wang, Y., Wang, L., Jiang, H., Zhang, C., Lu, M., Katakowski, M., Feldkamp, C.S., Chopp, M., 2003a. Statins induce angiogenesis, neurogenesis, and synaptogenesis after stroke. Ann. Neurol. 53, 743–751.

Chen, X.H., Iwata, A., Nonaka, M., Browne, K.D., Smith, D.H., 2003b. Neurogenesis and glial proliferation persist for at least one year in the subventricular zone following brain trauma in rats. J. Neurotrauma 20, 623–631.

Conover, J.C., Shook, B.A., 2011. Aging of the subventricular zone neural stem cell niche. Aging Dis. 2, 149–163.

Dao, T., Cheng, R.Y., Revelo, M.P., Mitzner, W., Tang, W., 2014. Hydroxymethylation as a novel environmental biosensor. Curr. Environ. Health Rep. 1, 1–10.

Feil, R., Fraga, M.F., 2011. Epigenetics and the environment: emerging patterns and implications. Nat. Rev. Genet. 13, 97–109.

Ficz, G., Branco, M.R., Seisenberger, S., Santos, F., Krueger, F., Hore, T.A., Marques, C.J., Andrews, S., Reik, W., 2011. Dynamic regulation of 5-hydroxymethylcytosine in mouse ES cells and during differentiation. Nature 473, 398–402.

Fitzsimons, C.P., van Bodegraven, E., Schouten, M., Lardenoije, R., Kompotis, K., Kenis, G., van den Hurk, M., Boks, M.P., Biojone, C., Joca, S., Steinbusch, H.W., Lunnon, K., Mastroeni, D.F., Mill, J., Lucassen, P.J., Coleman, P.D., van den Hove, D.L., Rutten, B.P., 2014. Epigenetic regulation of adult neural stem cells: implications for Alzheimer's disease. Mol. Neurodegener. 9, 9–25.

Freudenberg, J.M., Ghosh, S., Lackford, B.L., Yellaboina, S., Zheng, X., Li, R., Cuddapah, S., Wade, P.A., Hu, G., Jothi, R., 2012. Acute depletion of Tet1-dependent 5-hydroxymethylcytosine levels impairs LIF/Stat3 signaling and results in loss of embryonic stem cell identity. Nucleic Acids Res. 40, 3364–3377.

Jin, K., Galvan, V., Xie, L., Mao, X.O., Gorostiza OF, Bredesen, D.E., Greenberg, D.A., 2004a. Enhanced neurogenesis in Alzheimer's disease transgenic (PDGF-APPSw,Ind) mice. Proc. Natl. Acad. Sci. U. S. A. 101, 13363–13367.

Jin, K., Peel, A.L., Mao, X.O., Xie, L., Cottrell, B.A., Henshall, D.C., Greenberg, D.A., 2004b. Increased hippocampal neurogenesis in Alzheimer's disease. Proc. Natl. Acad. Sci. U. S. A. 101, 343–347.

Jin, K., Xie, L., Mao, X.O., Greenberg, D.A., 2006. Alzheimer's disease drugs promote neurogenesis. Brain Res. 1085, 183–188.

Kotani, S., Yamauchi, T., Teramoto, T., Ogura, H., 2008. Donepezil, an acetylcholinesterase inhibitor, enhances adult hippocampal neurogenesis. Chem. Biol. Interact. 175, 227–230.

Kuhn, H.G., Cooper-Kuhn, C.M., Boekhoorn, K., Lucassen, P.J., 2007. Changes in neurogenesis in dementia and Alzheimer mouse models: are they functionally relevant? Eur. Arch. Psychiatry Clin. Neurosci. 257, 281–289.

Lazarov, O., Mattson, M.P., Peterson, D.A., Pimplikar, S.W., van Praag, H., 2010. When neurogenesis encounters aging and disease. Trends Neurosci. 33, 569–579.

Leonard, B.W., Mastroeni, D., Grover, A., Liu, Q., Yang, K., Gao, M., Wu, J., Pootrakul, D., van den Berge, S.A., Hol, E.M., Rogers, J., 2009. Subventricular zone neural progenitors from rapid brain autopsies of elderly subjects with and without neurodegenerative disease. J. Comp. Neurol. 515, 269–294.

Lopez-Toledano, M.A., Shelanski, M.L., 2004. Neurogenic effect of beta-amyloid peptide in the development of neural stem cells. J. Neurosci. 24, 5439–5444.

Lue, L.F., Brachova, L., Walker, D.G., Rogers, J., 1996. Characterization of glial cultures from rapid autopsies of Alzheimer's and control patients. Neurobiol. Aging 17, 421–429.

Ma, D.K., Marchetto, M.C., Guo, J.U., Ming, G.L., Gage, F.H., Song, H., 2010. Epigenetic choreographers of neurogenesis in the adult mammalian brain. Nat. Neurosci. 13, 1338–1344.

Marlatt, M.W., Bauer, J., Aronica, E., van Haastert, E.S., Hoozemans, J.J., Joels, M., Lucassen, P.J., 2014. Proliferation in the Alzheimer hippocampus is due to microglia, not astroglia, and occurs at sites of amyloid deposition. Neural Plast. 2014 (1-13), 693851.

Ming, G.L., Song, H., 2011. Adult neurogenesis in the mammalian brain: significant answers and significant questions. Neuron 70, 687–702.

Monje, M.L., Mizumatsu, S., Fike, J.R., Palmer, T.D., 2002. Irradiation induces neural precursor-cell dysfunction. Nat. Med. 8, 955–962.

Mu, Y., Gage, F.H., 2011. Adult hippocampal neurogenesis and its role in Alzheimer's disease. Mol. Neurodegener. 6 (1-9), 85.

Navarro, A., Yin, P., Ono, M., Monsivais, D., Moravek, M.B., Coon, J.S., Dyson, M.T., Wei, J.J., Bulun, S.E., 2014. 5-hydroxymethylcytosine promotes proliferation of human uterine leiomyoma: a biological link to a new epigenetic modification in benign tumors. J. Clin. Endocrinol. Metab. 99, E2437–E2445.

Perry, E.K., Johnson, M., Ekonomou, A., Perry, R.H., Ballard, C., Attems, J., 2012. Neurogenic abnormalities in Alzheimer's disease differ between stages of neurogenesis and are partly related to cholinergic pathology. Neurobiol. Dis. 47, 155–162.

Politis, M., Lindvall, O., 2012. Clinical application of stem cell therapy in Parkinson's disease. BMC Med. 10, 1–10.

Riddle, D.R., Lichtenwalner, R.J., 2007. Neurogenesis in the adult and aging brain.

Szulwach, K.E., Li, X., Li, Y., Song, C.X., Han, J.W., Kim, S., Namburi, S., Hermetz, K., Kim, J.J., Rudd, M.K., Yoon, Y.S., Ren, B., He, C., Jin, P., 2011. Integrating 5-hydroxymethylcytosine into the epigenomic landscape of human embryonic stem cells. PLoS Genet. 7, e1002154.

Tahiliani, M., Koh, K.P., Shen, Y., Pastor, W.A., Bandukwala, H., Brudno, Y., Agarwal, S., Iyer, L.M., Liu, D.R., Aravind, L., Rao, A., 2009. Conversion of 5-methylcytosine to 5-hydroxymethylcytosine in mammalian DNA by MLL partner TET1. Science 324, 930–935.

Yamasaki, T.R., Blurton-Jones, M., Morrissette, D.A., Kitazawa, M., Oddo, S., LaFerla, F.M., 2007. Neural stem cells improve memory in an inducible mouse model of neuronal loss. J. Neurosci. 27, 11925–11933.

Yu, Y., He, J., Zhang, Y., Luo, H., Zhu, S., Yang, Y., Zhao, T., Wu, J., Huang, Y., Kong, J., Tan, Q., Li, X.M., 2009. Increased hippocampal neurogenesis in the progressive stage of Alzheimer's disease phenotype in an APP/PS1 double transgenic mouse model. Hippocampus 19, 1247–1253.

Zakharova, L., Mastroeni, D., Mutlu, N., Molina, M., Goldman, S., Diethrich, E., Gaballa, M.A., 2010. Transplantation of cardiac progenitor cell sheet onto infarcted heart promotes cardiogenesis and improves function. Cardiovasc. Res. 87, 40–49.

Zhang, P., Su, L., Wang, Z., Zhang, S., Guan, J., Chen, Y., Yin, Y., Gao, F., Tang, B., Li, Z., 2012. The involvement of 5-hydroxymethylcytosine in active DNA demethylation in mice. Biol. Reprod. 86 (1-9), 104.